Journal of Experimental Botany, Vol. 75, No. 8 pp. 2527–2544, 2024
https://doi.org/10.1093/jxb/erae025 Advance Access Publication 25 January 2024

RESEARCH PAPER

The genomic basis of nitrogen utilization efficiency and trait plasticity to improve nutrient stress tolerance in cultivated sunflower

Andries A. Temme[1,2,*], Kelly L. Kerr[1,3], Kristen M. Nolting[1], Emily L. Dittmar[1], Rishi R. Masalia[1], Alexander K. Bucksch[4], John M. Burke[1], and Lisa A. Donovan[1]

[1] Department of Plant Biology, University of Georgia, Athens, GA 30602, USA
[2] Department of Plant Breeding, Wageningen University & Research, 6700 HB Wageningen, The Netherlands
[3] School of Biological Sciences, University of Utah, Salt Lake City, UT 84112, USA
[4] School of Plant Sciences, University of Arizona, Tucson, AZ, USA

* Correspondence: Andries.Temme@wur.nl

Received 12 December 2022; Editorial decision 22 December 2023; Accepted 23 January 2024

Editor: Bertrand Muller, INRAE-Montpellier, France

Abstract

Maintaining crop productivity is challenging as population growth, climate change, and increasing fertilizer costs necessitate expanding crop production to poorer lands whilst reducing inputs. Enhancing crops' nutrient use efficiency is thus an important goal, but requires a better understanding of related traits and their genetic basis. We investigated variation in low nutrient stress tolerance in a diverse panel of cultivated sunflower genotypes grown under high and low nutrient conditions, assessing relative growth rate (RGR) as performance. We assessed variation in traits related to nitrogen utilization efficiency (NUtE), mass allocation, and leaf elemental content. Across genotypes, nutrient limitation generally reduced RGR. Moreover, there was a negative correlation between vigor (RGR in control) and decline in RGR in response to stress. Given this trade-off, we focused on nutrient stress tolerance independent of vigor. This tolerance metric correlated with the change in NUtE, plasticity for a suite of morphological traits, and leaf element content. Genome-wide associations revealed regions associated with variation and plasticity in multiple traits, including two regions with seemingly additive effects on NUtE change. Our results demonstrate potential avenues for improving sunflower nutrient stress tolerance independent of vigor, and highlight specific traits and genomic regions that could play a role in enhancing tolerance.

Keywords: Abiotic stress, GWAS, nutrient stress, plasticity, sunflower, tolerance.

Introduction

Rising population levels and climate change are increasing pressures on our global agricultural system to realize higher productivity on marginal lands (Ramankutty *et al.*, 2018). Additionally, demand for oilseed crops is projected to increase 90% by 2050 as compared with 2007 (Tilman *et al.*, 2011; Alexandratos and Bruinsma, 2012; Ramankutty *et al.*, 2018). To meet this challenge, the utility of increased fertilizer inputs is hampered by increasing costs of fertilizer and large negative

impacts of fertilizer on the environment (Vitousek *et al.*, 1997; Robertson and Vitousek, 2009). A more sustainable strategy is to improve the nutrient use efficiency of crops; that is, increase productivity per unit of available nutrients (Xu *et al.*, 2012). However, maintaining or even expanding productivity under low nutrient availability is a challenge.

Prior work on cultivated sunflower, a major oilseed crop, has revealed genotypic variation in tolerance to salt, flooding, and drought stress (Masalia *et al.*, 2018; Gao *et al.*, 2019; Temme *et al.*, 2020). Improvements in cultivated sunflower nutrient uptake and use efficiency can be key in meeting demand while maintaining or even reducing inputs. Prior work on sunflower nutrient stress response in a small number of genotypes showed a remarkable consistency in the performance ranking of genotypes across a range of nutrient levels (i.e. high performing genotypes tend to exhibit high performance across conditions, with lower performing genotypes exhibiting low performance across conditions; Bowsher *et al.*, 2017). Here, we more fully explore the effects of nutrient stress in cultivated sunflower and seek to identify key traits and genomic regions with a potential for improving nutrient stress tolerance.

Evaluating stress tolerance in the context of vigor (performance in benign conditions) is critical for improving resource use efficiency without associated decreases in productivity. Given the potential for a trade-off between vigor and the response to stress (e.g. Temme *et al.*, 2020), relating tolerance directly to stress response runs the risk of confounding tolerance with low vigor. Rather, by taking this negative relationship into consideration, we can score genotypes on being more or less tolerant than expected based on their vigor. Thus, tolerance is defined as performing better than would be expected based on this trade-off. This 'expectation–deviation tolerance' (ExDev-tolerance) metric makes it possible to isolate those traits or genomic regions that are directly involved in stress response independent of those underlying high performance (Temme *et al.*, 2020; Tran *et al.*, 2020). However, this raises the question of whether there are trade-offs (sensu Agrawal, 2020) in growth and development under stressful versus benign conditions and whether different suites of traits are associated with performance and tolerance.

Much progress has been made in understanding how nitrogen (N) use efficiency (growth per unit of available N) and its components, nitrogen uptake efficiency (efficiency of gathering N from soil) and nitrogen utilization efficiency (NUtE, growth per unit acquired N), can be improved (Han *et al.*, 2015; Tegeder and Masclaux-Daubresse, 2018; Swarbreck *et al.*, 2019). Realizing improved NUtE could involve efficient (re) distribution of N [and phosphorus (P)] to upper parts of the canopy, altering mass allocation, and adjusting leaf mass per area (LMA) and/or having more efficient photosynthetic machinery (Lammerts van Bueren and Struik, 2017). Understanding how these trait changes relate to ExDev-tolerance and NUtE is a potential avenue for improving tolerance independent of vigor.

An increased growth and development rate has been heavily selected for during domestication and crop improvement (Milla *et al.*, 2018). In improving plant traits for specific environments, the multivariate nature of trait covariation should be considered. Traits tend to covary due to a complex web of interactions (Poorter *et al.*, 2013, 2019, 2021). Identifying independent axes of trait variation can help focus improvement efforts to enhance tolerance independent of vigor. Improving overall nitrogen use efficiency will require integrating physiology and breeding to target the many inter-related (integrated) traits related to nitrogen uptake efficiency and NUtE.

Due to the multivariate nature of trait covariation, breeding efforts to select on particular traits can have unintended effects on other traits (Chebib and Guillaume, 2021; Svensson *et al.*, 2021). Due to pleiotropy or close linkage among traits, selection on one trait can affect others. Previous work on cultivated sunflower has shown a genomic landscape of trait co-localization where certain genomic regions are associated with a range of diverse traits (Masalia *et al.*, 2018; Temme *et al.*, 2020). By studying this landscape of trait co-localization, we can identify those regions with minimal effects on other traits in order to decouple and adjust this network of trait covariation. Thus, developing breeding strategies aimed at improving yields under a range of environmental conditions is facilitated by an understanding of the genomic regions underlying trait variation.

To determine the effects of low nutrient stress on key traits and genomic regions linked to improving nutrient stress tolerance in cultivated sunflower, we asked the following questions. (i) What is the relationship between vigor (growth under benign conditions) and the decline in performance in response to low nutrient stress? (ii) What is the relationship between NUtE and nutrient stress tolerance independent of vigor (ExDev-tolerance)? (iii) What is the effect of nutrient stress on traits potentially related to nutrient stress tolerance (e.g. morphology and leaf elemental content)? (iv) Which suites of trait variation and/or trait plasticity relate to ExDev-tolerance and vigor? (v) Can we identify shared and unique genomic regions associated with trait variation across a range of traits?

Materials and methods

Material

We grew a subset of 260 (out of 287) genotypes of the Sunflower Association Mapping (SAM) population (Mandel *et al.*, 2011, 2013). The SAM population includes both heterotic groups [i.e. male (RHA) and female (HA) lines] as well as both major market types [i.e. oil and non-oil (confectionery) lines]. The SAM population has been used extensively for genome-wide association studies (GWASs) (Masalia *et al.*, 2018; Gao *et al.*, 2019; Temme *et al.*, 2020; Stahlhut *et al.*, 2021) because of the substantial genetic/trait diversity contained within the population, relevant commercial uses, and the availability of whole-genome re-sequencing data for the entire population.

Growth conditions

In spring of 2016, we grew individuals of 260 SAM genotypes in a randomized block experimental design with two treatments, which each contained four replicates, in the Botany greenhouses at the University of

Georgia (Athens, GA, USA). Seeds were germinated in sand and transplanted to pots 7 d after sowing. Individuals were grown in 7.6 liter pots filled with a 3:1 mixture of sand and turface (Turface Athletics MVP, PROFILE Products, LLC, Buffalo Grove, IL, USA) to improve water-holding capacity. Two individuals per genotype were randomly assigned to each of four greenhouse bays, resulting in 2088 experimental plants. In each greenhouse bay, the two individuals of each genotype received either 80 g or 8 g of controlled-release fertilizer granules (Osmocote Plus 15-9-12; ScottsMiracle-Gro, Marysville, OH, USA) mixed into the upper soil layers at the beginning of the experiment to establish a favorable nutrient treatment and a broad-spectrum nutrient deficiency treatment, based on a previous study with a representative subset of 12 genotypes (Bowsher *et al.* 2017). The nutrient profile of the Osmocote Plus fertilizer pellets is 15.0% total N, 9.0% available phosphate, 12.0% soluble potash, 1.0% magnesium (Mg), 2.3% sulfur (S), 0.02% boron (B), 0.05% copper (Cu), 0.45% iron (Fe), 0.06% manganese (Mn), 0.02% molybdenum (Mo), and 0.05% zinc (Zn). We supplemented with calcium (Ca) using 5 ml of gypsum (Performance Minerals Corporation, Birmingham, AL, USA) and 5 ml of lime powder (Austinville Limestone, Austinville, VA, USA) per pot because prior experience has shown that Ca limitation results in developmental abnormalities under greenhouse conditions. Plants were initially watered to field capacity daily, and the watering regime was increased to twice daily to prevent water stress when temperatures and plant sizes increased. The treatments were immediately implemented upon transplanting to pots on 19 May 2016. Greenhouse air temperature and relative humidity were recorded in each of the four greenhouse bays every 10 min for the duration of the study. Across the four greenhouses, average air temperature ranged from 20.5 °C to 21.8 °C, maximum air temperature ranged from 26.7 °C to 28.4 °C, and minimum air temperature ranged from 11.8 °C to 17.0 °C. Across the four greenhouses, average relative humidity ranged from 63.2% to 72.8%, maximum relative humidity ranged from 90.8% to 92.2%, and minimum relative humidity ranged from 25.9% to 29.8%.

Plant harvest and trait measurements

Individual plants were tagged when they reached floral initiation (budding) (R1 stage) and harvested when they reached R2 stage, when the peduncle (flower stalk) had elongated to the point at which the primary bud was >1 cm above the nearest leaves (Schneiter and Miller, 1981). The process of harvesting plants at a specified developmental stage allowed us to identify the effect of nutrient stress on flowering time and early flower development while minimizing pot size constraints on biomass. Individuals reached the harvest stage between 19 d and 55 d after transplanting.

At harvest, plants were measured for height (to the nearest 0.5 cm from the base of the stem to the top of the stem), stem diameter (using calipers halfway between the soil and cotyledons), and chlorophyll content index (MC-100, Apogee Instruments, Inc., Logan, UT, USA) of the most recent fully expanded leaf (MRFEL). The MRFEL is an easy to define specific leaf in sunflower that standardizes leaf selection to a fully developed leaf toward the top of the plant. Generally, this leaf is in the upper 10% of the plant, with the number of underdeveloped leaves higher up on the stem varying by genotype. Plant biomass was then separated into the MRFEL, all other leaves, stem and branches [including bud(s)], and root. Roots were stored in a chilled environment and washed in order of harvest. Images were taken of the MRFEL at 300 dpi and of a single lateral root (near the soil surface but <2 mm diameter) at 600 dpi with a flatbed scanner (Canon CanoScan LiDE120) for use in determining dry LMA and specific root length (SRL). MRFEL scans were measured for area using ImageJ (Schneider *et al.*, 2012). Root scans were analyzed for SRL using RhizoVision Explorer v2.0.3 (Seethepalli *et al.*, 2021) to calculate total length, median root diameter, and branching frequency of the root sample. LMA was calculated by dividing the MRFEL weight (without petiole) by its measured area. SRL was calculated by dividing measured root length by the mass of the sampled root.

After oven drying at 60 °C for at least 48 h, dried samples were stored until weighing. Prior to weighing, all samples were redried at 60 °C for at least 2 h. After drying, lateral roots were separated from the taproot (up to the point at which the taproot and lateral roots had similar widths), and the primary and axillary buds were separated from the stem. The resulting biomass samples weighed separately for each individual were: the MRFEL, remaining leaves, stem, primary bud, axillary buds, taproot, lateral root, and SRL root sample. Biomass fractions including, root mass fraction (RMF), leaf mass fraction (LMF), and stem mass fraction (SMF), were calculated by dividing component parts by the total summed individual plant weight. RMF was further divided into tap and fine root mass as fractions of the whole-plant weight and root biomass.

After weighing, the MRFEL samples (without petiole) were pooled per genotype and treatment. Samples were coarse ground using a Wiley Mill (Thomas Scientific, Swedesboro, NJ, USA) and the resulting powder was homogenized. A 2 ml sample of leaf powder was then transferred to an Eppendorf tube and ground to a fine powder using a metal bead in a Tissuelyzer (Qiagen, Germantown, MD, USA). The finely powdered leaf tissue was then sent to Midwest Laboratories (Omaha, NE, USA) for inductively coupled plasma-MS (ICP-MS) analysis to determine the amounts of P, potassium (K), Ca, sodium (Na), S, Fe, Zn, Cu, Mg, Mn, and B, and, via the Dumas method, N, hereafter collectively referred to as elemental traits.

We assessed relative growth rate (RGR) as a performance metric of the plant. Following the approach of Hoffmann and Poorter (2002). RGR ($g_{plant}\ g_{plant}^{-1}\ d^{-1}$) was calculated as

$$\mathrm{RGR} = \frac{\ln(\text{biomass at harvest})}{\text{days to harvest}} \quad (1)$$

Equation 1 assumes exponential growth during the experiment and uniform size of the seedlings at transplanting to account for temporal differences in reaching the R2 stage under stress and non-limiting conditions.

NUtE ($g_{plant}\ g_{nitrogen}^{-1}\ d^{-1}$) was subsequently estimated as

$$\mathrm{NUtE} = \frac{\mathrm{RGR}}{\text{Leaf N fraction}} \quad (2)$$

This equation for NUtE assumes that leaf nitrogen content of the MRFEL is a good estimate for whole-plant nitrogen content.

Expectation–deviation-tolerance

Tolerance to nutrient stress was defined by Temme *et al.* (2020) for each genotype as the ExDev trait. This Ex-Dev trait is calculated as the residual per genotype to the fitted line between a genotype RGR in control and their difference in RGR under nutrient-limited conditions. The definition takes an expected negative linear relationship between RGR in control conditions and the decrease in RGR under stressed conditions into account. Visually, one can interpret the ExDev-tolerance trait as the distance of a genotype to the fitted line between RGR in control conditions and the decrease in RGR under stressed conditions (Temme *et al.*, 2020) independent of (i.e. after statistically accounting for) the effect of genotype vigor.

Statistical analysis

Results were analyzed using R (v4.1.2, R Core Team, 2021) in RStudio (RStudio Team, 2021). For all traits excluding leaf element content (due to lack of replication after pooling), we obtained genotype estimated

marginal means (using emmeans v1.7; Lenth, 2021) from a mixed model analysis (using LME4 v1.1-27.1; Bates *et al.*, 2015) taking genotype and treatment as fixed factors and greenhouse bay as a random factor. Wald's χ^2 test was used to test the significance of the main effects of genotype, treatment, and their interaction. Type 3 sums of squares were calculated (using car v3.0-12; Fox and Weisberg, 2011) given the presence of a significant interaction between genotype and treatment for many traits. For the pooled leaf biomass, two-sample *t*-tests were run to test for an effect of treatment on element content across genotypes. Genotype mean values for traits described herein are available in Supplementary Table S1 with trait naming conventions and descriptions (Supplementary Table S2).

Calculation of trait plasticity

To calculate trait plasticity per genotype, we took the difference in natural log-transformed values in control and stressed conditions. This proportional [can be converted to Δ% versus control via $e^{\Delta \ln(trait)}-1$] metric of plasticity has the additional benefit of being viewpoint agnostic. Only the sign of the natural log difference changes when it is viewed from the control versus stressed perspective. By using the natural log difference, a halving or doubling in trait value has the same magnitude of plasticity. We determined the level of correlation between mean trait values per genotype separately for trait values under control versus nutrient-limited conditions and for trait plasticities using Spearman correlation in corrr v0.4.3 (Kuhn *et al.*, 2020).

Given the level of expected covariation among traits, we explored major axes of variation within and across environments using principal component analysis (PCA) employing prcomp on scaled and centered trait values. To avoid biomass differences masking apparent responses between treatments, and to be able to relate major axes of trait variation and trait plasticity to performance, we selected a set of traits deemed putatively size independent (i.e. not directly reflecting any aspect of plant biomass) traits. These included chlorophyll content, fine root allocation (mass fraction and root fraction), LMA, LMF, RMF, SMF, and tap root allocation (mass fraction and root fraction). In addition to major axes of variation between treatments, we determined major axes of variation among genotypes within treatments and in trait plasticity for both size-independent traits and element content.

Trait heritability was estimated as both broad- (H^2) and narrow-sense heritability (h^2). Broad-sense heritability, as a measure of genotypic 'signal' compared with environmental 'noise', was calculated within each treatment on those traits with multiple replicates per genotype by fitting a mixed effects model with genotype as a random effect and greenhouse bay as a fixed effect. Subsequently, we calculated H^2 by dividing the genotypic variance by the sum of genotypic variance and residual variance divided by the number of replicates $\{H^2=V_g/[V_g+(V_e/n)]\}$. Narrow-sense heritability was calculated using the R package heritability (Kruijer *et al.*, 2015) that combines trait data (at the individual and genotypic mean level) with genotypic relatedness (based on pairwise genetic distance calculated using GEMMA; Zhou and Stephens, 2014). This approach allowed us to estimate h^2 for traits within each treatment and the plasticity between them.

Genome-wide association analyses

GWA analyses were carried out following Temme *et al.* (2020). Single nucleotide polymorphisms (SNPs) and annotation used were called as described in Hübner *et al.* (2018) and reordered based on the improved HA412-HOv2 sunflower genome assembly (Todesco *et al.*, 2020). Briefly, a collection of ~1.5 million high quality SNPs with minor allele frequency >5% and heterozygosity <10% were clustered into haplotypic blocks based on linkage disequilibrium (LD) estimated as *D'* (Gabriel *et al.*, 2002) using PLINK v1.9 (Chang *et al.*, 2015). This resulted in 9502 singleton SNPs and 20 652 co-inherited, multi-SNP haplotypic blocks across all 17 chromosomes that were used for the association analyses. Due to possible misordering of SNPs, these numbers are likely to be an overestimate since 'true' haplotypic blocks can be broken up by misplaced SNPs. GWA analyses were then carried out using GEMMA (Zhou and Stephens, 2014) on the full 1.5 million SNP set with our significance threshold (α=0.05) being adjusted for the number of observed haplotypic blocks (i.e. 0.05/20 652). When different traits had significant SNPs within the same haplotypic block (even if they were not the same SNPs), they were considered to co-localize to the same genomic region. Suggestive SNPs were defined as being in the top 0.01% of all SNPs (without meeting our significance threshold) for a trait and in a region that was significant for at least one other trait. All GWA analyses and visualizations were performed using our custom sunflower GWA pipeline (https://github.com/aatemme/Sunflower-GWAS-v2).

To connect observed instances of trait co-localization with pairwise trait–trait correlation values, we counted the number of significant and suggestive overlaps between all possible pairs of traits in each treatment and their plasticity, and related these counts to observed correlation coefficients. Because pairs of traits frequently shared zero regions, we fitted a negative binomial model with an |absolute| correlation coefficient as the predictor and the number of shared regions as the dependent variable using glm.nb from MASS v7.3-54 (Venables and Ripley, 2003).

Results

More vigorous genotypes experience a greater effect of nutrient limitation

Nutrient limitation generally had a significant impact on growth and development, with strong differences between genotypes (Table 1; Supplementary Fig. S1 for all individual traits). Under low nutrient stress, plants had a reduced developmental rate, delaying the onset of budding (R1 stage) by a median increase in days to reach R1 stage of 11.5%. Bud development was further slowed, resulting in a median increase in days to R2 of 16% (Fig. 1A inset), though genotypes differed widely from a 7% reduction to an 84% increase in time to reach this stage.

Despite the overall increase in time to reach R2, biomass was reduced by a median of 47% at R2 (Table 1; Fig. 1A). As genotypes developed, in both control and stressed conditions, those that took longer to reach R2 tended to have accumulated more biomass, though this effect was diminished under nutrient stress (Fig. 1A). This slower development time and reduced biomass accumulation due to low nutrient availability resulted in reduced RGR (Table 1; Fig. 1B). Genotypes with a higher RGR in control conditions (i.e. higher vigor) tended to have a higher RGR under low nutrient stress (Fig. 1B). Variation in the treatment effect on RGR across genotypes did not rise to the level of significance, as indicated by the lack of a G×T interaction on RGR (Table 1). This lack of a significant interaction could be the result of substantial within-genotype variation. However, when investigated across genotype means, our results do suggest that genotypes with overall higher vigor (higher RGR under control conditions) showed larger differences in growth between control and nutrient stress, indicating a possible trade-off between vigor and the effect of stress (P<0.001, Fig. 1C).

As we found this negative relationship between vigor and reduction in RGR, relating tolerance to only the difference in RGR due to stress runs the risk of confounding tolerance with

Table 1. Effect of nutrient stress on sunflower morphological and developmental traits

Traits	Control		Low nutrients		Plasticity (Δ%)		T	G	G×T
'Size' traits									
RGR (g_{plant} g_{plant}^{-1} d^{-1})	0.09	(0.04–0.11)	0.06	(0.03–0.08)	–31.1	(–49.64 to –6.4)	***	***	ns
Plant mass (g)	14.95	(2.43–61.08)	8.82	(1.93–26.84)	–42.6	(–75.04 to–68.18)	***	***	ns
Leaf mass (g)	8.42	(1.57–28.11)	3.42	(1.13–7.52)	–60.3	(–81.82 to –3.91)	***	***	***
Stem mass (g)	4.06	(0.36–25.81)	3.53	(0.26–16.3)	–14.1	(–71.32 to –272.18)	***	***	***
Reproductive tissue mass (g)	0.17	(0.06–0.53)	0.16	(0.08–0.34)	0	(–56.47 to –137.41)	***	***	***
Tap root mass (g)	1.03	(0.16–3.49)	0.51	(0.12–1.98)	–49.2	(–81.25 to –56.18)	***	***	ns
Lateral root mass (g)	1.27	(0.23–6.26)	1.14	(0.23–4.85)	–14.6	(–67.73 to –407.03)	***	***	ns
All root mass (g)	2.26	(0.39–8.67)	1.68	(0.41–5.68)	–32.4	(–69.78 to –280.73)	***	***	ns
All shoot mass (g)	12.48	(2.04–54.07)	7.03	(1.52–22.91)	–45	(–76.27 to –54.39)	***	***	***
Height (cm)	51.94	(17.37–118.5)	62	(15.75–126.12)	14.7	(–39.68 to –152.27)	***	***	***
Stem diameter (mm)	11.87	(6.37–19.62)	8.86	(5.44–13.46)	–25.6	(–52.98 to –17.63)	***	***	***
Lateral root diameter (mm)	0.44	(0.3–0.67)	0.41	(0.28–0.55)	–8.1	(–37.08 to –42.05)	***	***	ns
Development traits									
Days to R1 stage	26	(18.5–38.75)	28.77	(19.43–44.5)	11.5	(–15.55 to –65.52)	***	***	***
Days to R2 stage	30	(19.75–42.5)	35	(19.5–49.75)	16	(–7.09 to –84.26)	***	***	***
Days between R1 and R2	4.25	(1–11)	6.25	(1–13.75)	41.2	(–30.56 to –200)	***	***	***
Size-independent traits									
LMF (g_{leaves} g_{plant}^{-1})	0.57	(0.47–0.69)	0.39	(0.25–0.61)	–31	(–51.53 to –4.63)	***	***	***
SMF (g_{stem} g_{plant}^{-1})	0.26	(0.12–0.41)	0.4	(0.14–0.63)	48.7	(–7.29 to –120.6)	***	***	***
RMF (g_{roots} g_{plant}^{-1})	0.15	(0.09–0.23)	0.19	(0.11–0.28)	21.4	(–28.45 to –132.45)	***	***	ns
Root shoot ratio (g_{roots} g_{shoot}^{-1})	0.18	(0.1–0.55)	0.23	(0.13–0.57)	27.6	(–54.05 to –222.89)	***	***	ns
Tap root MF ($g_{tap\ root}$ g_{plant}^{-1})	0.07	(0.03–0.15)	0.06	(0.03–0.13)	–13.3	(–58.65 to –57.62)	***	***	ns
Fine root MF ($g_{fine\ root}$ g_{plant}^{-1})	0.08	(0.04–0.15)	0.13	(0.07–0.22)	49.2	(–15.57 to –255.51)	***	***	*
Tap root RF ($g_{tap\ root}$ g_{roots}^{-1})	0.46	(0.21–0.74)	0.32	(0.14–0.6)	–27.4	(–65.36 to –17.29)	***	***	*
Fine root RF ($g_{fine\ root}$ g_{roots}^{-1})	0.54	(0.26–0.79)	0.68	(0.4–0.86)	22.8	(–11.76 to –91.94)	***	***	*
LMA (g m^{-2})	36.1	(26.05–59.43)	37.17	(26.05–57.2)	2	(–22.84 to –41.97)	***	***	***
Leaf area ratio (m^2 g_{plant}^{-1})	0.02	(0.01–0.03)	0.01	(0–0.02)	–32.9	(–64.51 to –15.19)	***	***	**
Specific stem length (cm g^{-1})	14.72	(4.7–49.39)	18.22	(6.72–62.47)	30.4	(–61.34 to –194.28)	***	***	***
Specifc root length (m g^{-1})	9.64	(4.71–19.45)	10.55	(5.98–20.29)	9	(–45.05 to –207.29)	***	***	ns
Root branching frequency (mm^{-1})	0.47	(0.27–0.74)	0.5	(0.3–0.75)	5	(–45.71 to –110.83)	***	***	*
Chlorophyll content (index)	22.39	(12.39–36.85)	11.01	(6.95–18.23)	–50.2	(–73.6 to –-26.55)	***	***	***

Traits measured in our cultivated sunflower diversity panel with their median value (based on genotype means) and range (in parentheses) when grown under control (i.e. high nutrient) and low nutrient (10% of control) conditions, as well as an estimate of their plasticity (trait adjustment) between treatments. Plasticity was calculated as the difference in natural log-transformed values [ln(low nutrients)–ln(control)] but converted here to Δ% versus control [via $e^{\Delta ln(trait)}$–1] for ease of interpretation. Asterisks indicate significance [Wald's χ^2 of genotype (G), treatment (T), and their interaction (G×T)]. ns, non-significant; *P<0.05; **P<0.01; ***P<0.001.

low vigor. By fitting a linear relationship between the difference in RGR and and vigor for each genotype, performance relative to the overall expectation can be estimated as the residual from this fitted line. We define this residual as the ExDev-tolerance of each genotype, allowing us to score them as being more or less tolerant than expected based on their vigor.

Expectation–deviation-tolerance is positively correlated with the change in nitrogen utilization efficiency

Genotypes with a higher leaf nitrogen content at harvest (R2 stage) had a lower RGR, under both control and low nutrient conditions (Fig. 2A inset). Given that RGR and leaf N content both changed in response to low nutrient availability, we used growth rate per unit leaf nitrogen as a metric for NUtE. Genotypes with the highest NUtE in control conditions tended to remain the highest under nutrient stress (Fig. 2A). Moreover, nearly all genotypes increased NUtE, indicated by positive ΔNUtE, though the extent of this varied among genotypes (Fig. 2B). Strikingly, there was a strong positive relationship between the increase in NUtE and ExDev-tolerance (Fig. 2C). Genotypes that exhibited greater than expected increases in NUtE (independent of their actual NUtE) tended to have a higher ExDev-tolerance (i.e. a smaller reduction in RGR than expected), suggesting a possible role for NUtE in low nutrient tolerance.

Nutrient stress has large impacts on diverse plant traits and leaf elemental content

Under control and nutrient-stressed conditions, genotypes varied substantially in their traits and plasticity in traits (Table 1;

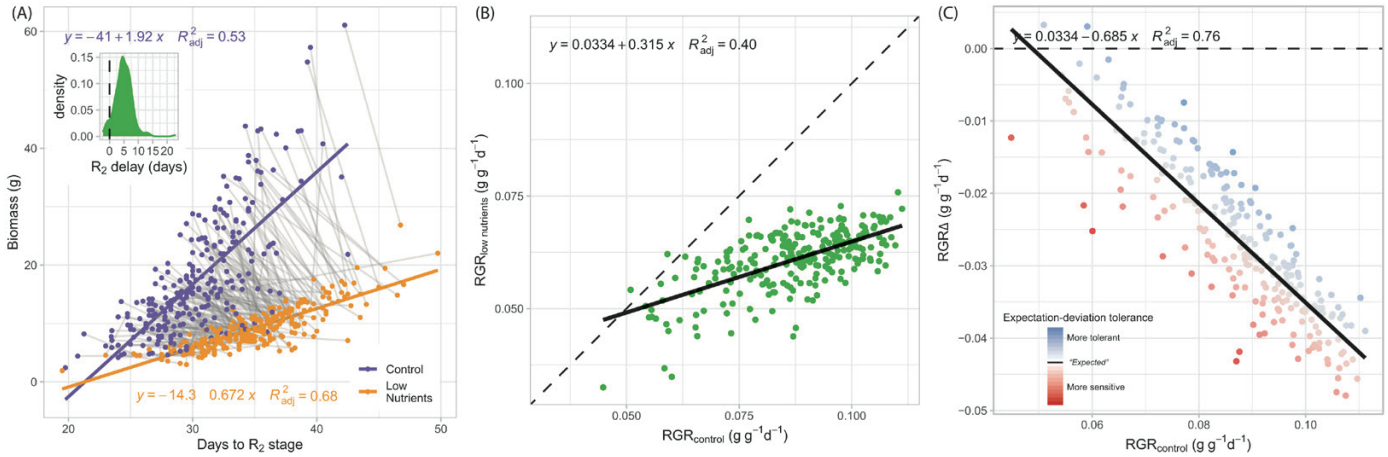

Fig. 1. Effect of nutrient limitation on development time, relative growth rate (RGR), and the effect of stress. Plants under low nutrient stress had reduced biomass and RGR, and took longer to reach the R2 stage. (A) Relationship between days to reach the R2 (early budding) stage and biomass at that time under control conditions (purple) and nutrient limitation treatment (orange). Genotypes (colored dots, *n*=260) are connected between treatments with gray lines. Generally, nutrient limitation delayed the R2 stage. The inset panel shows the distribution of the delay in reaching the R2 stage. (B) Relationship between RGR under control conditions and RGR under nutrient limitation across all genotypes (green dots, *n*=260). The dotted line shows the 1:1 relationship. (C) RGR in control versus the difference in RGR in nutrient-limited conditions. Genotypes (*n*=260) are colored by their residual from the fitted line. This ExDev-tolerance metric shows more sensitive (red) and more tolerant (blue) genotypes. Equations describe the best-fit line with the R^2_{adj} of that model.

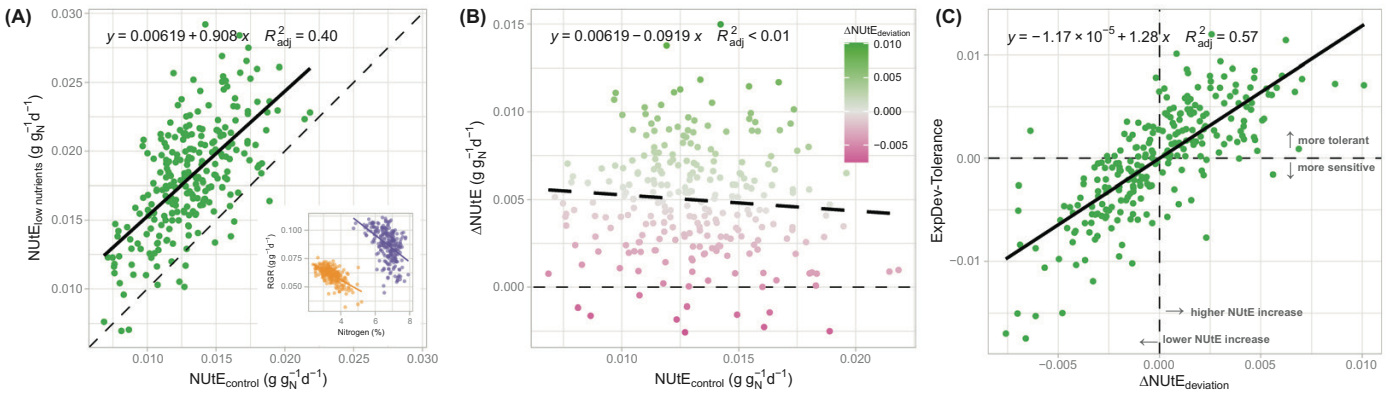

Fig. 2. Nitrogen utilization efficiency (NUtE) and its relation to nutrient stress tolerance. (A) Relationship between NUtE [estimated as growth rate per unit leaf nitrogen ($g_{biomass}$ g_N^{-1} d^{-1})] in control conditions and NUtE in low limited conditions. The dotted line shows the 1:1 relationship. The inset shows the relationship between leaf N content and RGR, used to calculate NUtE (control, purple; low nutrients, orange). (B) Relationship between NUtE in control conditions and the change in NUtE from control to low nutrient conditions. (C) Relationship between the deviation from the mean NUtE increase and ExDev-tolerance.

Supplementary Fig. S1). Overall, in the low nutrient treatment, more biomass was allocated to roots, leading to a median of 21.4% increased RMF as compared with the control; this was primarily driven by an increase in fine RMF. In addition to roots, more biomass was also allocated to stem tissue (Table 1). Low nutrient stress also resulted in alterations in plant morphology where the MRFEL became smaller and thicker or denser (i.e. increased LMA), roots became thinner or less dense (i.e. increased SRL), and stems became thinner despite an increase in height (i.e. increased specific stem length). Chlorophyll content of the leaf was drastically reduced, by a median of −50%, tracking the large effect of low nutrient availability on leaf elemental composition (Table 1; Supplementary Fig. S1).

With the exception of Na and Mn, nutrient stress generally had large and significant (between treatments) effects on leaf element content (Table 2; Supplementary Fig. S1). Leaf N decreased by 49%, P by 36%, and K by 15%. Ca content increased dramatically, with a 123% increase under low nutrient conditions versus the control, although it should be noted that we supplied additional Ca as gypsum and lime, and as such Ca was abundantly available in both treatments. Additionally, the Mg content increased by 32%. However, while the concentration of Ca and Mg increased, the total amount in the leaf remained largely the same for Ca and was lower for Mg (Supplementary Fig. S2) due to a concomitant decrease in leaf mass.

Table 2. Effect of nutrient stress on sunflower leaf elemental content

Trait	Control		Low nutrients		Plasticity (Δ%)		P(T)
Nitrogen (%)	6.8	(4.74–7.92)	3.41	(2.39–5.21)	–48.9	(–63.86 to –22.7)	***
NUtE (g_{plant} g_N^{-1} d^{-1})	0.01	(0.01–0.02)	0.02	(0.01–0.03)	38.9	(–20.14 to –115.55)	***
Phosphorus (%)	0.48	(0.32–0.76)	0.3	(0.21–0.43)	–36.4	(–62.07 to –9.37)	***
Potassium (%)	4.91	(3.46–6.85)	4.07	(2.67–6.03)	–15.3	(–40.88 to –12.09)	***
Sulfur (%)	0.68	(0.42–1.77)	0.45	(0.24–1.38)	–32.1	(–63.75 to –21.82)	***
Calcium (%)	1.07	(0.68–1.76)	2.43	(1.08–4.73)	123.3	(42.86 to –290.35)	***
Magnesium (%)	0.43	(0.3–0.8)	0.58	(0.24–0.92)	32	(–35.14 to –117.65)	***
Manganese (ppm)	328	(133–878)	320	(160–914)	–1.1	(–67.53 to –155.29)	ns
Copper (ppm)	24	(13–40)	14	(7–40)	–42.9	(–74.19 to –73.91)	***
Iron (ppm)	120	(76–468)	81	(49–443)	–30	(–85.5 to –340)	***
Boron (ppm)	78	(47–143)	73	(38–111)	–6.8	(–45.68 to –69.64)	***
Zinc (ppm)	55	(33–96)	42	(20–115)	–22.2	(–63.33 to –187.18)	***

Leaf element content of the most recent fully expanded leaf measured in bulked samples on our sunflower diversity panel. Values shown are the median content across genotypes (with range in parentheses) when grown under control (i.e. high nutrient) and nutrient-limited (10% of high nutrients) conditions, as well as the plasticity (as Δ%) between them. Plasticity was calculated as the difference in natural log-transformed values [ln(low nutrients)–ln(control)] but converted here to Δ% versus control [via $e^{\Delta ln(trait)}$–1) for ease of interpretation. Element content is shown on a mass basis (g g^{-1}). Since individual leaves per genotype were bulked, asterisks indicate significance (based on a *t*-test) of nutrient limitation treatment. ns, non-significant; *P<0.05; **P<0.01; ***P<0.001.

Major axes of trait variation/plasticity correlate with expectation–deviation-tolerance and vigor

To investigate trait relationships in the context of nutrient stress tolerance, and to determine if they differ from traits related to high vigor, we sought to determine the correspondence between tolerance, performance, and variation in broad multivariate suites of traits. Across both treatments, >60% of the variation in size-independent traits (Fig. 3A) and >60% of the variation in leaf elemental content (Fig. 3B) could be captured in the first two principal components (PCs). Differences between treatments largely followed PC1, with a shift towards below-ground resource allocation (i.e. decreased chlorophyll, LMF, and LAR, increased RMF, and investment in fine roots). Leaf element content was highly correlated between treatments, with reduced levels of N, P, K, S, and Cu coupled with increased levels of Ca and Mg under low nutrient availability.

To connect trait variation to differences in performance and tolerance, we adopted a within-treatment and plasticity-between-treatments approach. We related major axes of trait variation in (putatively) size-independent traits and leaf elemental traits under control and low nutrient conditions, along with trait plasticity between treatments to RGR and ExDev-tolerance. We found that PC1 of size-independent traits under control and low nutrient conditions was closely correlated with RGR in those environments (Table 3). ExDev-tolerance was significantly correlated with the first two PCs of the plasticity in size-independent traits, but the relationship with PC1 was more robust (Table 3; Fig. 4B). Multivariate leaf elemental content was likewise correlated with RGR as well as ExDev-tolerance. More specifically, variation in PC2 of leaf elemental content was associated with RGR and, to a lesser extent, ExDev-tolerance (Fig. 4D).

Genotypes with a suite of size-independent trait adjustments related to a greater decrease in LAR and a greater increase in the fraction of biomass allocated to fine roots (at the expense of tap root) were more tolerant (Supplementary Table S3; Fig. 4A, B). In terms of elemental content, genotypes that had higher leaf N, P, and K content had higher ExDev-tolerance (Supplementary Table S3; Fig. 4C, D). For a full picture of trait loadings onto principal components, see Supplementary Table S3.

Multiple genomic regions associated with trait variation and plasticity to nutrient stress

Variation of all measured traits (Table 4) in control and low nutrients, and trait plasticity between treatments, could be associated with 215 unique, putatively independent genomic regions (based on LD; Supplementary Fig. S3; Supplementary Table S4). The number of significantly associated regions per trait (Table 4) varied widely and tended to be lower for trait plasticity across treatments as compared with trait values within treatments. Our finding of >20 distinct regions for S content in close proximity to each other (Supplementary Fig. S4) may reflect localized misordering in the genome assembly; in reality, these regions may very well be grouped together. Thus, our finding of 215 independent regions should be viewed as an overestimate; there are likely to be fewer major effect regions involved in variation in these traits, though there are probably other regions too with effects below the level of detectability. Note also that for traits with no significant G×T (Table 1) when contrasting all individual plants, at the level of genotype averages we find occasional significant regions. While false positives for trait plasticity could be a reason, this could also

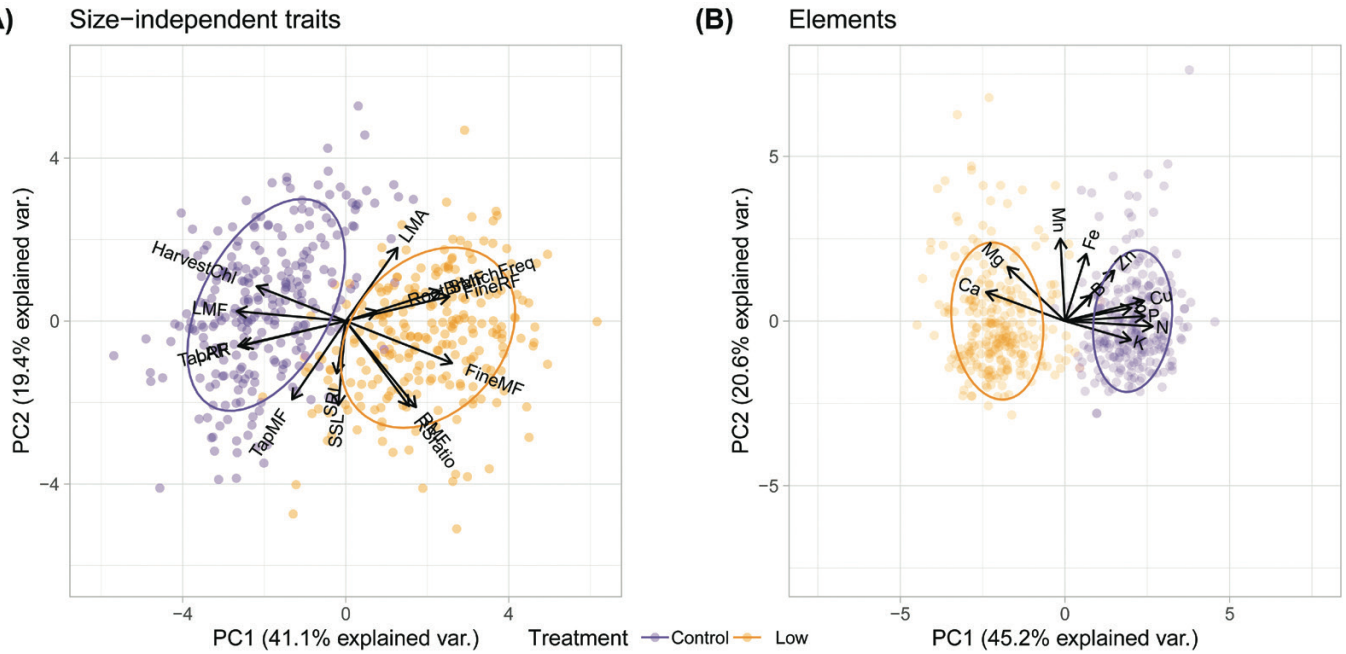

Fig. 3. Multivariate trait shifts in response to low nutrient availability in sunflower. Principal component analysis (PCA) reveals correlated trait adjustments to low nutrient stress for (A) putatively size-independent traits [chlorophyll content, fine root allocation (mass fraction and root fraction), LMA, LMF, RMF, SMF, and tap root allocation (mass fraction and root fraction)], SRL, and root branching frequency, and (B) leaf elemental traits (N, P, K, S, Ca, Mg, Mn, Cu, Fe, B, and Zn) in control (high nutrient) treatment (purple) and low nutrient treatment (orange).

Table 3. Relationship of sunflower relative growth rate and ExDev-tolerance with correlated suites of size-independent and leaf ionomic traits

Trait suite	Treatment	PCA	RGR control	RGR low nutrients	ExDev-tolerance
			R^2	R^2	R^2
Size-independent	Control	PC1	**0.51*** **	0.2***	
		PC2		0.02*	
	Low nutrients	PC1	0.33***	**0.45*** **	0.14***
		PC2			
	Plasticity	PC1		0.11***	**0.23*** **
		PC2	0.06***		0.02*
Elements	Control	PC1	0.07***		
		PC2	0.15***	0.08***	
	Low nutrients	PC1	0.05***	0.03**	
		PC2	0.22***	**0.32*** **	**0.12*** **
	Plasticity	PC1		0.02*	
		PC2	0.07***	0.16***	0.09***

R^2 and significance of the ordinary least squares regression of the PC1 and PC2 values of the putatively size-independent traits [chlorophyll content, fine root allocation (mass fraction and root fraction), LMA, LMF, RMF, SMF, tap root allocation (mass fraction and root fraction)], and elemental traits (B, Ca, Cu, Fe, Mg, Mn, N, P, K, S, Zn) under control (high nutrients) and low nutrient (10% of control) conditions, as well as the plasticity in trait values between treatments. Highlighted in bold are the model fits RGR and ExDev-tolerance against the principal components with the highest explanatory power for vigor and tolerance for each trait. *P<0.05, **P<0.01, ***P < 0.001.

reflect a fairly weak genetic effect that is drowned out by individual level variability.

Per trait, the overlap in regions significantly (or suggestively) associating with variation in both treatments and its plasticity was low (Table 4). Across traits, 51 regions (across 13 of the 17 chromosomes, Supplementary Fig. S5) were significantly associated with multiple trait–environment combinations, though this number rises to 178 regions if we include suggestive associations (i.e. regions having SNPs in the top 0.01% of P-values and significant for at least one other trait) (Supplementary Table S5; Supplementary Fig. S6 for a complete picture of trait and region co-localization). Several genomic hotspots

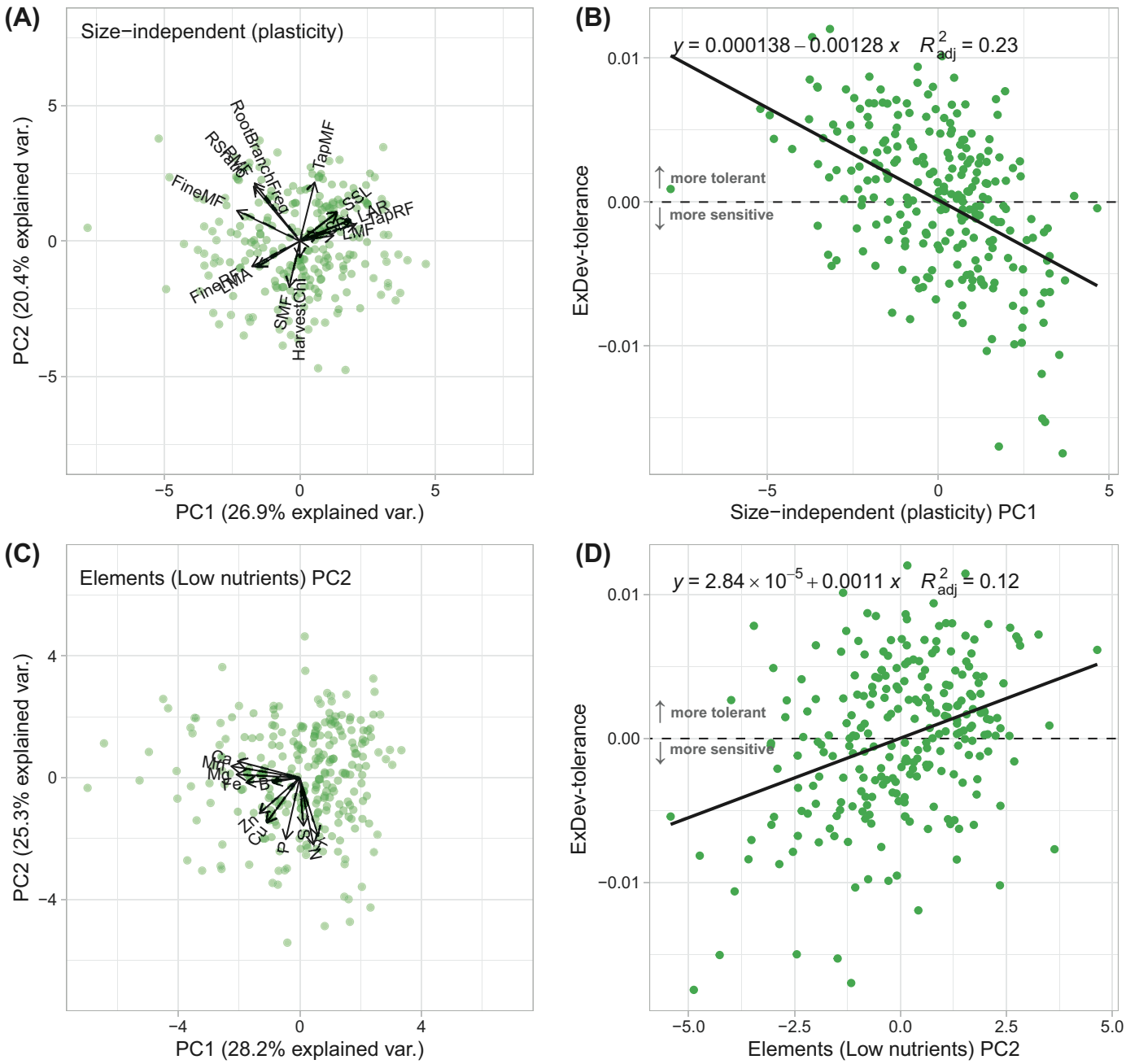

Fig. 4. Major axes of trait plasticity and leaf elemental content are correlated with ExDev-tolerance. (A) Principal component analysis (PCA) of the plasticity in (putatively) size-independent traits in response to nutrient limitation (genotypes *n*=246). (B) Relationship between genotypes (green points) loading on PC1 of the plasticity in size-independent traits and genotypic nutrient stress ExDev-tolerance. (C) PCA of leaf elemental content under low nutrient availability (genotypes *n*=259). (D) Relationship between genotypes (green points) loading on PC2 of leaf elemental content in low nutrients and genotype nutrient stress tolerance.

associating with multiple traits could be found (Supplementary Table S6). Of these hotspots, the region associating with variation in the largest number of traits was region 17-09, which was significantly associated with nine traits (related to aspects of root mass, S and Mn content, and development time) and a diverse set of 54 suggestive traits. Unfortunately, this region was quite large (>50 Mb) and contained 699 genes, making it difficult to distinguish between the pleiotropic effects of a single locus and close linkage of multiple functional variants. In contrast, the second largest hotspot, region 03-06, was significantly associated with eight biomass-related traits and contained only seven genes. Unfortunately only three of the seven genes had known or putative functions (*Putative EH domain, EF-hand domain pair protein*, *Putative protein kinase TKL-CTR1-DRK-2*

Table 4. Genomic associations and trait heritability at control and low nutrients of mean value of traits and their plasticities

Trait	Control				Low nutrients				Plasticity			Region overlap		
	H^2	h^2	Signif. (unique) regions	Sugg. regs.	H^2	h^2	Signif. (unique) regions	Sugg. regs.	h^2	Signif. (unique) regions	Sugg. regs.	Ctrl. and Low	Ctrl. and Plast.	Low and Plast.
ExDev-tolerance	Cross-treatment trait	–	0.5 ± 0.09	0 (0)	9	Cross-treatment trait	Cross-treatment trait							
ΔNUtE-dev.	Cross-treatment trait	–	0.5 ± 0.09	2 (0)	10	Cross-treatment trait	Cross-treatment trait							
RGR (g_{plant} g_{plant}^{-1} d^{-1})	0.74	0.08 ± 0.075	0 (0)	11	0.73	0.08 ± 0.04	0 (0)	20	0.07 ± 0.075	0 (0)	5	0 (3)	0 (0)	0 (1)
Plant mass (g)	0.90	0.76 ± 0.09	5 (0)	30	0.89	0.73 ± 0.055	5 (1)	31	0.1 ± 0.09	1 (0)	12	0 (11)	0 (4)	0 (1)
Leaf mass (g)	0.90	0.74 ± 0.11	1 (0)	34	0.87	0.69 ± 0.055	1 (0)	24	0.18 ± 0.11	0 (0)	10	0 (10)	0 (3)	0 (3)
Stem mass (g)	0.90	0.75 ± 0.09	14 (8)	27	0.91	0.76 ± 0.05	5 (1)	23	0.09 ± 0.09	0 (0)	19	1 (8)	0 (3)	0 (1)
Reproductive tissue mass (g)	0.65	0.29 ± 0.07	3 (3)	9	0.57	0.16 ± 0.065	2 (2)	4	0.06 ± 0.07	2 (1)	7	0 (1)	0 (3)	0 (1)
Tap root mass (g)	0.80	0.61 ± 0.065	3 (0)	21	0.84	0.67 ± 0.06	7 (5)	19	0.06 ± 0.065	1 (0)	10	0 (6)	0 (4)	0 (0)
Lateral root mass (g)	0.85	0.65 ± 0.075	1 (1)	21	0.82	0.61 ± 0.07	5 (0)	18	0.08 ± 0.075	1 (0)	10	0 (4)	0 (2)	0 (2)
All root mass (g)	0.86	0.7 ± 0.07	5 (0)	15	0.84	0.65 ± 0.065	6 (2)	15	0.06 ± 0.07	3 (1)	7	0 (2)	0 (1)	0 (0)
All shoot mass (g)	0.90	0.75 ± 0.095	5 (0)	35	0.90	0.74 ± 0.05	4 (0)	27	0.13 ± 0.095	0 (0)	13	1 (10)	0 (6)	0 (0)
Height (cm)	0.88	0.69 ± 0.085	0 (0)	29	0.89	0.7 ± 0.055	0 (0)	17	0.08 ± 0.085	0 (0)	11	0 (7)	0 (6)	0 (2)
Stem diameter (mm)	0.85	0.65 ± 0.12	1 (0)	34	0.81	0.59 ± 0.07	1 (0)	28	0.19 ± 0.12	0 (0)	9	0 (12)	0 (6)	0 (1)
Lateral root diameter (mm)	0.25	0.07 ± 0.04	1 (1)	5	0.58	0.22 ± 0.08	1 (1)	9	0.02 ± 0.04	0 (0)	7	0 (0)	0 (0)	0 (1)
Days to R1 stage	0.88	0.74 ± 0.095	2 (2)	30	0.88	0.75 ± 0.045	0 (0)	23	0.11 ± 0.095	1 (0)	2	0 (13)	0 (0)	0 (0)
Days to R2 stage	0.87	0.72 ± 0.12	2 (2)	30	0.90	0.77 ± 0.045	1 (0)	24	0.15 ± 0.12	1 (0)	7	0 (11)	0 (0)	0 (2)
Days between R1 and R2	0.62	0.32 ± 0.075	5 (5)	6	0.71	0.47 ± 0.08	7 (7)	10	0.07 ± 0.075	1 (1)	15	0 (1)	1 (1)	0 (2)
LMF (g_{leaves} g_{plant}^{-1})	0.85	0.55 ± 0.16	1 (0)	14	0.87	0.77 ± 0.04	3 (0)	25	0.27 ± 0.16	0 (0)	19	0 (2)	0 (3)	0 (11)
SMF (g_{stem} g_{plant}^{-1})	0.86	0.61 ± 0.04	1 (0)	19	0.88	0.73 ± 0.05	4 (2)	15	0.02 ± 0.04	0 (0)	12	1 (2)	0 (3)	0 (2)
RMF (g_{roots} g_{plant}^{-1})	0.76	0.3 ± 0.075	0 (0)	7	0.67	0.24 ± 0.075	0 (0)	12	0.09 ± 0.075	1 (1)	4	0 (1)	0 (1)	0 (0)
Root shoot ratio (g_{roots} g_{shoot}^{-1})	0.60	0.28 ± 0.075	8 (8)	10	0.62	0.27 ± 0.085	1 (1)	11	0.08 ± 0.075	2 (1)	7	0 (3)	1 (1)	0 (1)
Tap root MF ($g_{tap\ root}$ g_{plant}^{-1})	0.79	0.09 ± 0.05	4 (2)	6	0.81	0.09 ± 0.045	4 (4)	7	0.04 ± 0.05	0 (0)	13	2 (0)	0 (2)	0 (1)
Fine root MF ($g_{fine\ root}$ g_{plant}^{-1})	0.60	0.07 ± 0.07	2 (2)	12	0.63	0.21 ± 0.075	0 (0)	19	0.07 ± 0.07	1 (1)	9	0 (6)	0 (3)	0 (6)
Tap root RF ($g_{tap\ root}$ g_{roots}^{-1})	0.68	0.33 ± 0.05	1 (0)	16	0.73	0.36 ± 0.085	1 (0)	9	0.04 ± 0.05	1 (0)	6	0 (6)	0 (1)	0 (1)
Fine root RF ($g_{fine\ root}$ g_{roots}^{-1})	0.68	0.33 ± 0.07	1 (0)	16	0.73	0.36 ± 0.085	1 (0)	9	0.06 ± 0.07	0 (0)	6	0 (6)	0 (1)	0 (0)
LMA (g m^{-2})	0.70	0.39 ± 0.06	3 (3)	19	0.72	0.45 ± 0.08	2 (2)	24	0.05 ± 0.06	0 (0)	7	1 (6)	0 (2)	0 (2)

Table 4. Continued

Trait	Control				Low nutrients				Plasticity			Region overlap		
	H^2	h^2	Signif. (unique) regions	Sugg. regs.	H^2	h^2	Signif. (unique) regions	Sugg. regs.	h^2	Signif. (unique) regions	Sugg. regs.	Ctrl. and Low	Ctrl. and Plast.	Low and Plast.
Leaf area ratio (m^2 g_{plant}^{-1})	0.78	0.09 ± 0.08	0 (0)	19	0.85	0.11 ± 0.05	3 (1)	19	0.08 ± 0.08	1 (1)	14	0 (4)	0 (2)	0 (1)
Specific stem length (cm g^{-1})	0.76	0.5 ± 0.085	2 (2)	17	0.86	0.7 ± 0.055	8 (6)	20	0.09 ± 0.085	0 (0)	8	0 (5)	0 (1)	0 (2)
Specifc root length (m g^{-1})	0.35	0.1 ± 0.02	0 (0)	11	0.39	0.12 ± 0.07	1 (1)	12	0 ± 0.02	2 (1)	7	0 (2)	0 (2)	0 (4)
Root branching frequency (mm^{-1})	0.43	0.12 ± 0.06	1 (1)	7	0.36	0.09 ± 0.06	2 (2)	5	0.04 ± 0.06	1 (1)	7	0 (0)	0 (2)	0 (1)
Chlorophyll content (index)	0.79	0.54 ± 0.1	0 (0)	9	0.87	0.71 ± 0.055	2 (2)	6	0.11 ± 0.1	2 (2)	8	0 (1)	0 (1)	0 (1)
Nitrogen (%)	–	0.5 ± 0.105	2 (1)	21	–	0.5 ± 0.11	1 (1)	22	0.13 ± 0.105	0 (0)	13	0 (2)	0 (1)	0 (5)
NUtE (g_{plant} g_N^{-1} d^{-1})	–	0.48 ± 0.075	0 (0)	18	–	0.49 ± 0.175	1 (0)	23	0.07 ± 0.075	4 (3)	1	0 (7)	0 (0)	0 (1)
Phosphorus (%)	–	0.43 ± 0.05	1 (1)	4	–	0.42 ± 0.18	2 (2)	3	0.03 ± 0.05	0 (0)	4	0 (0)	0 (0)	0 (0)
Potassium (%)	–	0.62 ± 0.085	0 (0)	14	–	0.61 ± 0.165	2 (1)	9	0.08 ± 0.085	1 (1)	8	0 (0)	0 (1)	0 (2)
Sulfur (%)	–	0.19 ± 0.165	20 (16)	9	–	0.41 ± 0.13	21 (17)	10	0.32 ± 0.165	3 (2)	16	5 (1)	0 (2)	1 (2)
Calcium (%)	–	0.37 ± 0.075	0 (0)	11	–	0.55 ± 0.18	1 (1)	20	0.09 ± 0.075	5 (5)	7	0 (2)	0 (2)	0 (3)
Magnesium (%)	–	0.36 ± 0.095	1 (1)	18	–	0.42 ± 0.17	7 (7)	1	0.12 ± 0.095	2 (1)	13	0 (0)	0 (2)	0 (0)
Manganese (ppm)	–	0.38 ± 0.11	10 (6)	19	–	0.48 ± 0.175	5 (3)	14	0.13 ± 0.11	1 (1)	11	0 (1)	0 (2)	0 (0)
Copper (ppm)	–	0.53 ± 0.075	1 (0)	13	–	0.61 ± 0.175	3 (3)	7	0.07 ± 0.075	0 (0)	12	0 (3)	0 (1)	0 (1)
Iron (ppm)	–	0.51 ± 0.09	12 (8)	8	–	0.41 ± 0.16	4 (2)	8	0.11 ± 0.09	0 (0)	10	0 (0)	0 (1)	0 (2)
Boron (ppm)	–	0.32 ± 0.145	1 (1)	5	–	0.34 ± 0.17	1 (1)	5	0.23 ± 0.145	0 (0)	10	0 (0)	0 (1)	0 (2)
Zinc (ppm)	–	0.07 ± 0.07	0 (0)	6	–	0.17 ± 0.11	0 (0)	11	0.06 ± 0.07	8 (8)	10	0 (2)	0 (1)	0 (1)

Shown is the broad-sense (H^2) and narrow sense (h^2) heritability of all measured traits at control conditions, under low nutrient stress, and the plasticity between treatments. For traits where only genotype means were available, only h^2 could be calculated. Additionally the number of significant (Signif.) genomic regions per trait (with those unique to that trait/treatment combination in parentheses) and the number of suggestive regions (Sugg. Regs.), SNPs in that region in the top 0.01% of association strength and significant for at least one other trait. For region overlap, the number of overlapping significant (suggestive regions in parentheses) genomic regions per trait is shown in control (cont.) and low nutrients, cont. and plasticity (plast.), and low nutrients and plast. ExDev-tolerance and ΔNUtE deviation lack values in Control and Plasticity as these traits combine results from control and low nutrient treatment in their calculation; as such, they are only presented at low nutrients.

family, and *Putative Late embryogenesis abundant protein, LEA_2 subgroup*), highlighting the difficulty of determining candidate genes from GWAS results alone.

As one might expect, at the genomic level, we saw a reflection of the correlated nature of variation in traits (Fig. 5). Strongly positively or negatively correlated traits tended to share a greater number of genomic regions with significant and/or suggestive SNPs associated with those traits. Indeed, in both treatments, we found a significant relationship between bivariate trait correlation strength and the number of shared genomic regions associating with those traits. While the shape of this relationship was comparable between control (high nutrients) and low nutrient treatment, highly correlated trait plasticities (a compound trait, calculated across both treatments) tended to share a lower number of genomic regions (Fig. 5D).

We found no significant genomic regions directly underlying nutrient stress tolerance (i.e. having a lower than expected—based on vigor—reduction in RGR). However, we did find eight regions with suggestive associations for tolerance that were significant for key traits identified by our PCAs (e.g. root mass allocation and NUtE; Table 3; Fig. 5). For the genotypic deviations from expected (average) NUtE increase (Fig. 2B), a key trait involved in tolerance in this study (Fig. 2C), we found two significant genomic regions (Fig. 6A). These regions on chromosome 1 (01-01) and chromosome 17 (17-13) contained 176 genes and 8 genes, respectively.

Focusing on these latter two regions, we found that genotypes that carry the minor allele in both regions (generally homozygous due to our filtering) tended to have a higher NUtE increase under low nutrient conditions as compared with those carrying the major allele (Fig. 6A). Interestingly, the six genotypes with the minor alleles of both regions had (on average) an even further improved NutE, suggesting an additive effect for these regions (Fig. 6B). While it should be noted that these regions were not significantly associated with ExDev-tolerance, when plotted on the relationship between RGR in control and the decline in RGR (similar to Fig. 1C), it can be seen that the genotypes that carry the minor allele for either or both regions tend towards being more tolerant than would be expected based on their vigor (Fig. 6C).

Discussion

Improving our understanding of crop nutrient stress tolerance will aid in developing varieties capable of high performance on marginal lands and/or with reduced inputs (Good *et al.*, 2004). Here, we sought to determine the traits and genomic regions involved in low nutrient stress tolerance in cultivated sunflower, one of the world's most important oilseed crops.

The greater the vigor the harder the fall

Similar to prior findings for salt stress (Temme *et al.*, 2020; Tran *et al.*, 2020), plants with higher vigor (high RGR) under control conditions tended to have the best overall performance (i.e. higher RGR) under nutrient-limited conditions. However, these same genotypes tended to exhibit a greater reduction in RGR under nutrient-limited conditions. Thus, genotypes with high performance under nutrient limitation versus those with a low effect of nutrient limitation on performance represent largely non-overlapping sets, making it difficult to identify 'tolerance' on the basis of performance *per se*. To address this challenge, our definition of tolerance accounts for the negative relationship between vigor and the decrease in RGR due to nutrient limitation. In doing so, genotypes are scored by their deviation from their expected reduction in growth, given their vigor. This ExDev-tolerance exhibited moderate heritability across genotypes, showing the potential for improving genotypes by focusing on this tolerance metric, though we did not identify any specific genomic regions associated with this trait,

Low nutrient stress slowed sunflower's rate of development, with nutrient limitation exhibiting a particularly strong effect on the number of days to reach R2 (early bud development). More specifically, we found an average 11.5% increase in the time to reach R1 (onset of bud development) and a 40% increase in the time to reach the following R2 (Table 1). In an agricultural setting, such a slowdown in development could result in plants running into unfavorable environmental conditions (e.g. later season heat, drought) (Kazan and Lyons, 2016). Interestingly, this slowdown in development was highly heterogeneous across genotypes, with a small fraction exhibiting more rapid development (up to 15.5% shorter time to R1) while others extended their development time by as much as 65.5%. The low heritability of genotypic plasticity in developmental time and the lack of overlap in genomic regions associated with developmental rate traits in both environments suggests difficulty in optimizing a cultivar for a range of environments. However, given the high heritability of development time (Table 4) within environments, it may be possible to optimize cultivars for particular environments.

Higher nitrogen utilization efficiency is associated with greater expectation–deviation-tolerance

Relating growth to N uptake is of particular interest due to the essential role N plays in multiple physiological processes, including the conversion of CO_2 into biomass. Improving a plant's capacity to acquire and use N more efficiently may be the key to improving performance in poor nutrient conditions (Han *et al.*, 2015; Tegeder and Masclaux-Daubresse, 2018; Swarbreck *et al.*, 2019). Similar to results from ryegrass (Zhao *et al.*, 2020), sunflower was found to generally increase NutE under nutrient limitation (Fig. 2A). Moreover, in contrast to RGR, the magnitude of this increase was unrelated to NUtE under benign conditions. However, we did find substantial genotypic variation in the magnitude of this NUtE increase (Fig. 2B).

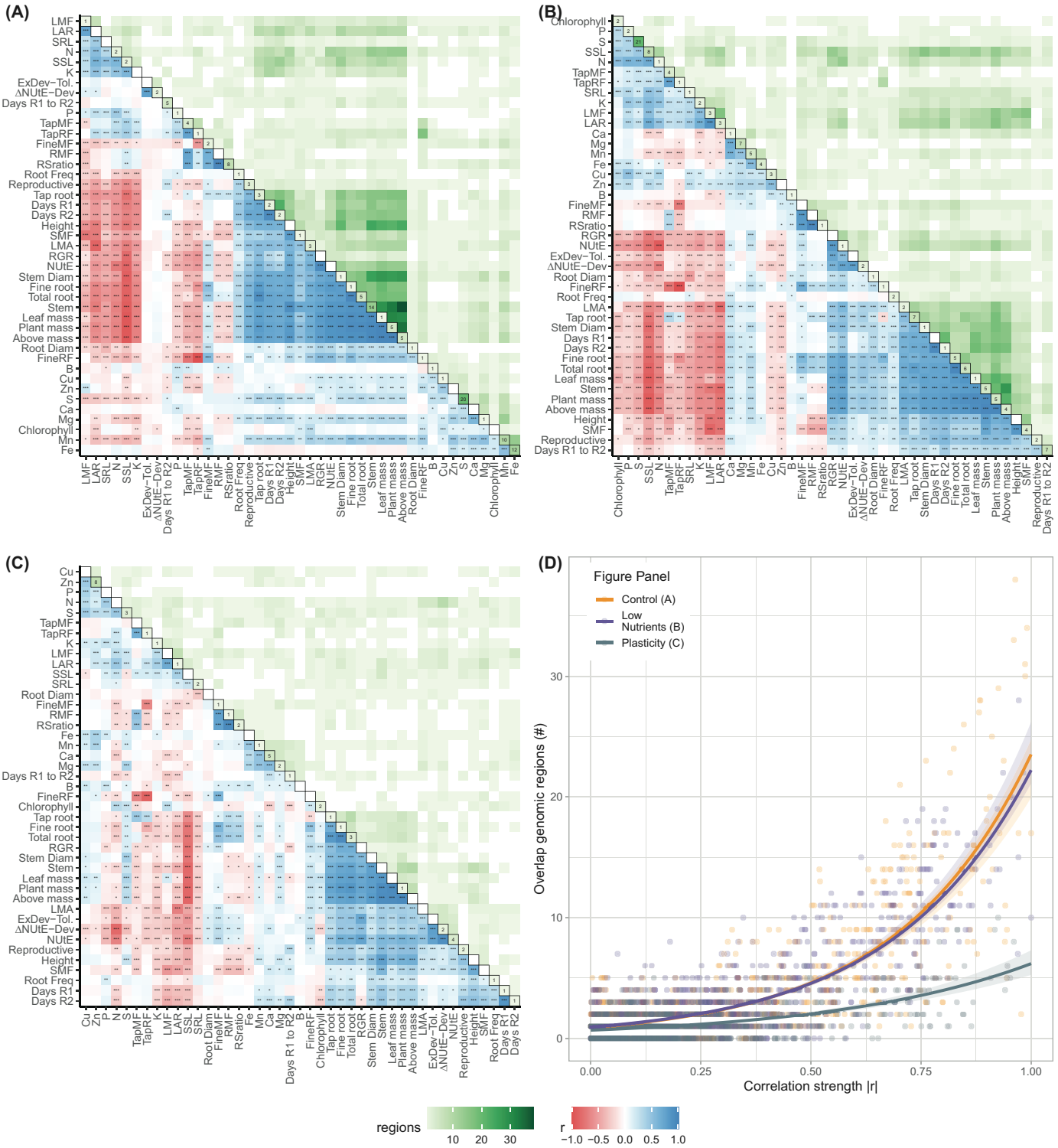

Fig. 5. Sunflower trait correlations and genomic co-localization. (A) Spearman correlation matrix of phenotypic and elemental traits in our cultivated sunflower diversity panel under control (control conditions; lower diagonal) and the number of overlapping genomic regions (at the suggestive level, upper diagonal). The total number of significant regions listed per trait on the diagonal. Traits are ordered by hierarchical clustering in each panel so that closely correlated traits are close together. (B) Correlation of traits and overlapping genomic regions under low nutrient conditions. (C) Correlation and overlap in genomic regions for trait plasticity values between treatments [ln(control)–ln(stress)]. (D) Logistic regression of absolute pairwise trait–trait correlation coefficient and the number of overlapping genomic regions. Correlation values range from –1 (red) to 1 (blue). Asterisks in tiles indicate the significance of correlations: **P*<0.05, ***P*<0.01, ****P*<0.001.

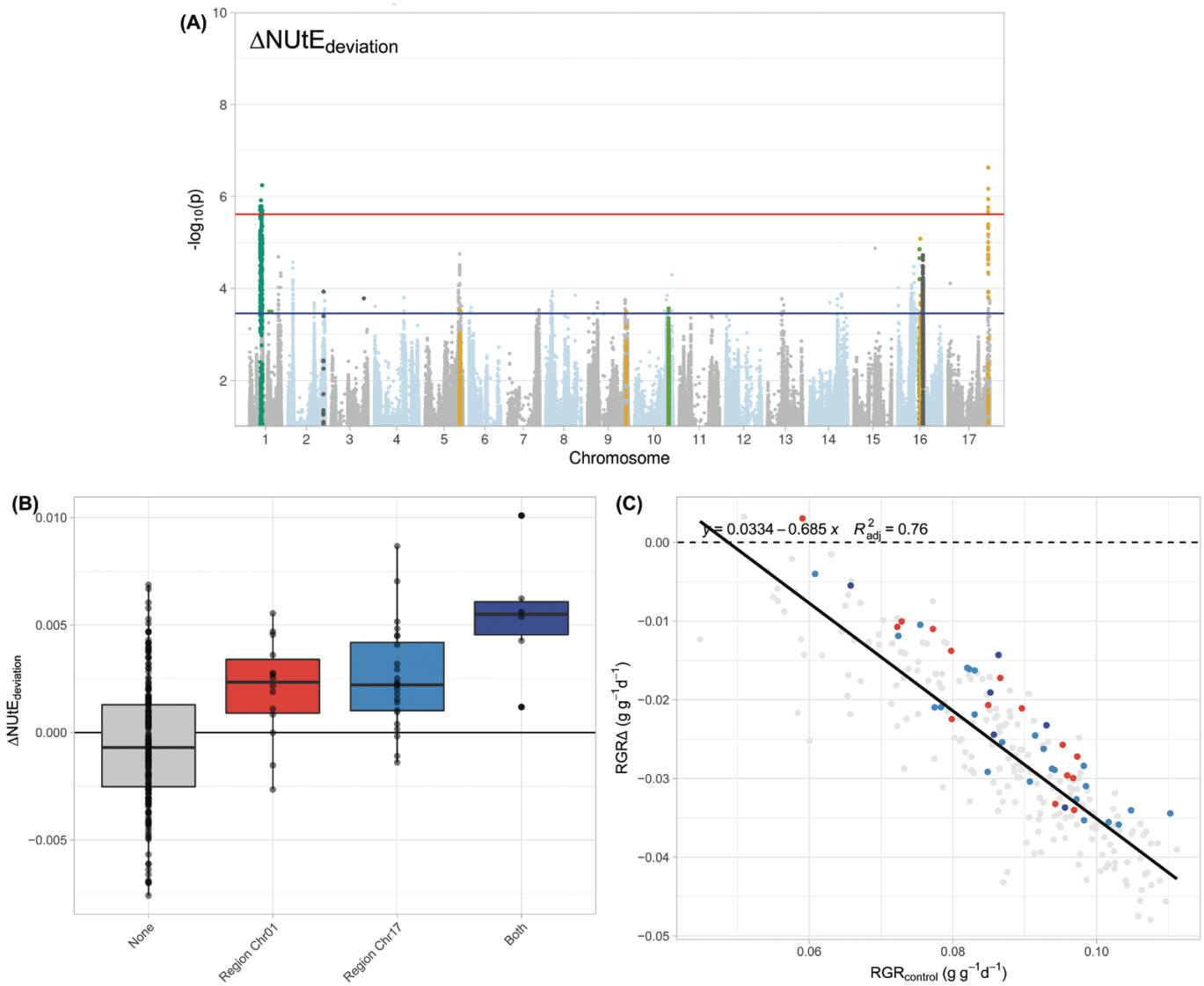

Fig. 6. Regions associated with the change in NUtE and their expected effect on ExDev-tolerance. (A) Manhattan plot of the deviation from expected increase in NUtE across genotypes. Two haplotypic regions, 01-01 and 17-29, are significantly associated with this trait (SNPs above the red line). Several other regions show suggestive associations that co-localize with other traits (highlighted SNPs above the blue line). (B) Deviation in NUtE increase under low nutrient conditions (negative values=smaller increase than expected, positive values=larger increase than expected) and minor allele status for regions 01-01 and 17-29 (the most significant SNP within each haplotypic region was selected as the tag SNP for that region). Genotypes with the minor allele in either region tend to be more tolerant, with a seemingly additive effect for the few genotypes that have both minor alleles. (C) Visualization of the genotypes carrying the minor allele for regions 01-01 and 17-29 (colors correspond to those used in B) and where they fall on a plot of ExDev-tolerance.

While our measures of growth (RGR) and NUtE are not wholly independent, relating our measure of ExDev-tolerance to genotype change in NUtE highlights the importance of NUtE in determining the response to low nutrient stress (Xu *et al.*, 2012; Han *et al.*, 2015). Indeed, genotypes that exhibit greater increases in NUtE under stress tend to exhibit greater ExDev-tolerance. Thus, improving NUtE could be a strategy for improving nutrient tolerance in sunflower without reducing vigor. For NUtE in control and nutrient-stressed conditions and genotype deviation from the overall NUtE increase, we found that moderate narrow-sense heritability and several genomic regions were associated with variation in NUtE under low nutrient stress and plasticity in NUtE (Table 4). Interestingly, for the deviation in NUtE, we found two regions with seemingly additive effects (Fig. 6), showing the potential for trait optimization via selection.

Vigor and tolerance are correlated with distinct multivariate suites of traits and trait plasticity

Similar to other species (Weih *et al.*, 2018; Meyer *et al.*, 2019), low nutrient stress leads to a host of trait changes in cultivated

sunflower, with broad multivariate changes in trait expression across environments (Fig. 3). Over 60% of the variation in size-independent traits and leaf elemental content across control and low nutrient stress were captured by the first two PCs in each case. Similarly, variation in traits within treatments and plasticity between treatments could be simplified into a limited number of major axes of variation (Supplementary Fig. S3). These strong multivariate axes of covariation illustrate the difficulty in isolating changes in individual traits to produce novel trait combinations (Walsh and Blows, 2009).

With strong covariation among trait variation within treatments as well as plasticity between them, relating single traits to tolerance would be a gross oversimplification. Rather, we related the major axes of variation in size-independent traits and leaf element content to Ex-Dev-tolerance and RGR. In both control treatment and low nutrient stress treatment, RGR was correlated with a suite of traits related to carbon uptake (LAR, LMF, and SSL). ExDev-tolerance was, however, correlated with a suite of trait plasticities, with genotypes exhibiting a greater decrease in LAR and a greater increase in the fraction of biomass allocated to fine roots at the expense of tap root being more tolerant overall (Supplementary Table S3; Fig. 4A, B). Results from cotton show this same connection between RSA and nitrate uptake efficiency (Iqbal *et al.*, 2020). Moreover, comparably with our findings for salt stress (Temme *et al.*, 2020), traits related to ExDev-tolerance differ from those related to vigor, indicating that in principle it could be possible to combine high tolerance with high vigor.

Further comparisons with our findings for salt stress (Temme *et al.*, 2020) and with a large multienvironment screening of cultivated sunflower cold×nutrient×drought response (Mangin *et al.*, 2017) shows that trait plasticity can be a key factor in stress tolerance. In both the past salt experiment (Temme *et al.*, 2020) and the current nutrient experiment we found some generality in higher ExDev-tolerance associated with plasticity in allocation. Under salt stress, a greater increase (i.e plasticity) in whole-plant RMF and in the proportion of fine roots in root mass were linked with higher ExDev-tolerance. Here, for nutrients, we find similar results for root plasticity. Due to the nature of the stress, at the leaf elemental level, we see contrasting responses where under salt stress leaf Na and K content and ratio were linked with higher ExDev-tolerance whereas here for nutrients it was maintenance of N, P, and K content under nutrients stress that was linked with ExDev-tolerance. Contrasting with broad ecological multispecies patterns of trait variation under resource-poor environments (Wright *et al.*, 2004), we found no connection between ExDev-tolerance and SLA under both salt and nutrient stress. In the field, Mangin *et al.* (2017) found a negative relationship between oil yield and the capacity to plastically adjust traits. However, comparably with our findings, here the existence of high-yielding, stress-tolerant varieties indicates the potential for combining these factors through breeding and that there is no inherent trade-off that would preclude this.

Multiple genomic regions impact trait variation and plasticity

A large number of genomic regions were involved in trait variation under control and low nutrient conditions. Interestingly, similar to findings in maize, we find additional genomic regions associated with trait plasticity (Gage *et al.*, 2017; Kusmec *et al.*, 2017), often distinct from those involved in variation in either treatment (Supplementary Fig. S4). The often large size of regions identified, containing many genes, makes functional inferences at the level of individual genes difficult (Supplementary Table S4). While one of the largest genomic regions can be attributed to the relatively recent conversion of sunflowers to a hybrid crop (particularly the branching locus on chromosome 10; Mandel *et al.*, 2013), it stands to reason that with a larger panel of genotypes our LD-based region sizes would shrink, lowering the possible number of genes involved (Korte and Farlow, 2013). However, despite this limitation, some interesting trends and key genes could be found in the regions of interest.

For developmental rate, days to reach R2 (i.e. bud formation) was significantly associated with region 04_01 under control conditions. This region of two genes contains a 'Transcription factor interactor and regulator AUX-IAA family' gene, suggesting a specific mechanism related to auxin transport involved in development rate (Sauer *et al.*, 2013). Below-ground, region 08_14, significant for plasticity in RMF and containing 14 genes, included a 'Transcription factor MYB-HB-like family' gene. This family of transcription factors is known to be involved in several processes including response to stress and development (Ambawat *et al.*, 2013). Root morphology, as reflected in root branching frequency, was associated with two regions (02_03 and 02_06) under low nutrient conditions. These regions contained 51 and 35 genes, respectively, with both harboring a putative gene in the RLK/Pelle family of kinases. This family of kinases is involved in a host of processes including development (Gish and Clark, 2011). The *Putative protein kinase RLK-Pelle-CrRLK1L-1 family* in region 02_06 is of a type linked to cell expansion (Nissen *et al.*, 2016), suggesting a mechanism for altered branching frequency. Two key genomic regions on chromosomes 1 and 17 could be directly linked to NUtE increases with ostensibly additive effects. Region 17-14 (eight genes) contained a '*LAZY1*' gene, which is known to be involved in auxin transport (Dong *et al.*, 2013). However, extreme care should be taken in overinterpreting these results as far more genes of unknown function are also contained in these significant regions and, due to LD, any of these could also be a causal variant.

In comparing overlaps in associated genomic regions among traits, we found that traits that tended to covary more strongly tended to share a higher number of genomic regions associated with those traits (Fig. 5D). In interpreting this result, care should be taken since some of these correlations could be due to the fact that trait pairs could be compound traits that share underlying

physiological processes or have mathematical dependencies. This connection between phenotypes/traits, also called trait integration, or the study of an organism's multivariate phenotype, is an ongoing avenue of research (Pigliucci and Preston, 2004; Messier *et al.*, 2017). Experiments have shown that trait adjustments to the environment rarely happen in isolation and that through understanding a genotype's integrated phenotype responses to the environments can be better understood (Richards *et al.*, 2006). Due to pleiotropy, based either on close linkage or shared genetic pathways, selecting on one trait or trait plasticity has the potential to impact many others (Wagner and Zhang, 2011; Mural *et al.*, 2021; Svensson *et al.*, 2021). In a multienvironment study, Mangin *et al.* (2017) found distinct suites of trait plasticities associated with cold, drought, and nutrient stress, indicating the potential for optimizing genotypes for particular environments. A full atlas of trait and trait plasticity associations on the sunflower genome would be a key resource showing possibilities of selecting on particular traits and the consequences of that across multiple environments.

Conclusion

Different abiotic stresses (e.g. drought, salinity, or low nutrient stress) exhibit different modes of action, and tolerance to these stresses is thus conferred by different sets of traits. However, here, in cultivated sunflower, we find overall responses to low nutrient stress that reflect results from prior work on salinity stress (Temme *et al.*, 2020). Across genotypes, those with the highest vigor (i.e. growth in benign conditions) tend to remain the best performers under low nutrient stress. However, these same high vigor genotypes also suffer the most under low nutrient conditions (i.e. they exhibit the greatest decrease in RGR). In defining tolerance, we therefore took this vigor/stress effect relationship into account. Genotypes with a smaller decrease than expected based on their vigor are thus viewed as being more stress tolerant, and vice versa. For nutrient stress, we found that this ExDev-tolerance metric was positively correlated with NUtE. More specifically, those genotypes that exhibited an above average increase in NUtE are those that have a high ExDev-tolerance. In addition to NUtE, we found that ExDev-tolerance was to a suite of multivariate trait plasticities where genotypes that exhibit a greater decrease in LAR, a greater increase in the fraction of biomass allocated to fine roots, and less to tap root were more tolerant of low nutrient conditions. Numerous genomic regions were found to be associated with trait variation and plasticity. While we found many regions associated with variation in multiple traits, unique regions for traits were found as well. Thus, while there are generally more regions involved in variation in multiple traits, observed instances of genomic regions affecting only individual traits in this experiment leave open the possibility of genetically decoupling certain trait combinations in the interest of exploring novel phenotypic space. Genotypic variation in ExDev-tolerance, a close tie between ExDev-tolerance and NUtE, multivariate suites of traits correlated with ExDev-tolerance, and a host of potential genomic targets show the potential for enhancing low nutrient stress tolerance in cultivated sunflower.

Supplementary data

The following Supplementary data are available at *JXB* online.

Table S1. Data for all genotypes and trait values exhibited in this study.

Table S2. Trait naming conventions in raw data, GWAS output, and as used in the body of the text with their units and description.

Table S3. PC1 and PC2 loadings under control and low nutrient-stressed conditions and plasticity (companion to Table 3 and Fig. 4).

Table S4. Output from GEMMA analyses of all significant SNPs and their associated trait and treatment combination.

Table S5. Putative genes contained in significant regions based on LD.

Table S6. List of significant genomic regions and associated significant/suggestive traits.

Fig. S1. Detailed per trait response to nutrient limitation.

Fig. S2. Graphical description of whole-leaf calcium and magnesium amounts.

Fig. S3. LD plots per chromosome.

Fig. S4. All Manhattans.

Fig. S5. Significant regions on genome haplotype block.

Fig. S6. Trait co-localization per chromosome.

Fig. S7. All PCAs (companion to Table 3).

Acknowledgements

We thank K. Bettinger, M. Boyd, K. Tarner, UGA greenhouse staff, the sunflower undergraduate army, and numerous past and present members of the Donovan and Burke labs for their help during the experiment. Special thanks to the reviewers for their valuable feedback.

Author contributions

AAT, JMB, and LAD: conceptualization; AAT and KLK: design and carrying out the experiment; AKB: assisting with analysis of the root images; AAT: analyzing all results with input from KMN and ELD; RRM: contributing to the GWAS pipeline. AAT wrote the first manuscript draft with input from all authors.

Conflict of interest

The authors have no conflicts to declare.

Funding

This work was supported by a grant from the NSF Plant Genome Research Program (IOS-1444522) to JMB and LAD.

Data availability

Data are available in the supplementary data and in Zenodo: https://doi.org/10.5281/zenodo.10137780 (Temme *et al.*, 2024).

References

Agrawal AA. 2020. A scale-dependent framework for trade-offs, syndromes, and specialization in organismal biology. Ecology **101**, e02924.

Alexandratos N, Bruinsma J. 2012. World agriculture towards 2030/2050: the 2012 revision. ESA Working paper No. 12-03. Rome: FAO.

Ambawat S, Sharma P, Yadav NR, Yadav RC. 2013. MYB transcription factor genes as regulators for plant responses: an overview. Physiology and Molecular Biology of Plants **19**, 307–321.

Bates D, Mächler M, Bolker B, Walker S. 2015. Fitting linear mixed-effects models using lme4. Journal of Statistical Software **67**, 1–48.

Bowsher AW, Shelby KC, Ahmed I, Krall E, Reagan DJ, Najdowski MN, Donovan LA. 2017. Genotype rankings for nutrient stress resistance are unrelated to stress severity in cultivated sunflower (*Helianthus annuus* L.). Journal of Agronomy and Crop Science **203**, 241–253.

Chang CC, Chow CC, Tellier LC, Vattikuti S, Purcell SM, Lee JJ. 2015. Second-generation PLINK: rising to the challenge of larger and richer datasets. GigaScience **4**, 7.

Chebib J, Guillaume F. 2021. Pleiotropy or linkage? Their relative contributions to the genetic correlation of quantitative traits and detection by multitrait GWA studies. Genetics **219**, iyab159.

Dong Z, Jiang C, Chen X, *et al*. 2013. Maize LAZY1 mediates shoot gravitropism and inflorescence development through regulating auxin transport, auxin signaling, and light response. Plant Physiology **163**, 1306–1322.

Fox J, Weisberg S. 2011. An R companion to applied regression, 2nd edn. Thousand Oaks, CA: Sage.

Gabriel SB, Schaffner SF, Nguyen H, *et al*. 2002. The structure of haplotype blocks in the human genome. Science **296**, 2225–2229.

Gage JL, Jarquin D, Romay C, *et al*. 2017. The effect of artificial selection on phenotypic plasticity in maize. Nature Communications **8**, 1348.

Gao L, Lee JS, Hübner S, Hulke BS, Qu Y, Rieseberg LH. 2019. Genetic and phenotypic analyses indicate that resistance to flooding stress is uncoupled from performance in cultivated sunflower. New Phytologist **223**, 1657–1670.

Gish LA, Clark SE. 2011. The RLK/Pelle family of kinases. The Plant Journal **66**, 117–127.

Good AG, Shrawat AK, Muench DG. 2004. Can less yield more? Is reducing nutrient input into the environment compatible with maintaining crop production? Trends in Plant Science **9**, 597–605.

Han M, Okamoto M, Beatty PH, Rothstein SJ, Good AG. 2015. The genetics of nitrogen use efficiency in crop plants. Annual Review of Genetics **49**, 269–289.

Hoffmann WA, Poorter H. 2002. Avoiding bias in calculations of relative growth rate. Annals of Botany **90**, 37–42.

Hübner S, Bercovich N, Todesco M, *et al*. 2018. Sunflower pan-genome analysis shows that hybridization altered gene content and disease resistance. Nature Plants **5**, 54–62.

Iqbal A, Qiang D, Zhun W, Xiangru W, Huiping G, Hengheng Z, Nianchang P, Xiling Z, Meizhen S. 2020. Growth and nitrogen metabolism are associated with nitrogen-use efficiency in cotton genotypes. Plant Physiology and Biochemistry **149**, 61–74.

Kazan K, Lyons R. 2016. The link between flowering time and stress tolerance. Journal of Experimental Botany **67**, 47–60.

Korte A, Farlow A. 2013. The advantages and limitations of trait analysis with GWAS: a review. Plant Methods **9**, 29.

Kruijer W, Boer MP, Malosetti M, Flood PJ, Engel B, Kooke R, Keurentjes JJB, van Eeuwijk FA. 2015. Marker-based estimation of heritability in immortal populations. Genetics **199**, 379–398.

Kuhn M, Jackson S, Cimentada J. 2020. corrr: correlations in R. R package version 0.4.3. https://corrr.tidymodels.org.

Kusmec A, Srinivasan S, Nettleton D, Schnable PS. 2017. Distinct genetic architectures for phenotype means and plasticities in *Zea mays*. Nature Plants **3**, 715–723.

Lammerts van Bueren ET, Struik PC. 2017. Diverse concepts of breeding for nitrogen use efficiency. A review. Agronomy for Sustainable Development **37**, 50.

Lenth RV. 2021. emmeans: Estimated Marginal Means, aka Least-Squares Means. R package version 1.7.0. https://CRAN.R-project.org/package=emmeans.

Mandel JR, Dechaine JM, Marek LF, Burke JM. 2011. Genetic diversity and population structure in cultivated sunflower and a comparison to its wild progenitor, *Helianthus annuus* L. Theoretical and Applied Genetics **123**, 693–704.

Mandel JR, Nambeesan S, Bowers JE, Marek LF, Ebert D, Rieseberg LH, Knapp SJ, Burke JM. 2013. Association mapping and the genomic consequences of selection in sunflower. PLoS Genetics **9**, e1003378.

Mangin B, Casadebaig P, Cadic E, *et al*. 2017. Genetic control of plasticity of oil yield for combined abiotic stresses using a joint approach of crop modelling and genome-wide association. Plant, Cell & Environment **40**, 2276–2291.

Masalia RR, Temme AA, Torralba N de L, Burke JM. 2018. Multiple genomic regions influence root morphology and seedling growth in cultivated sunflower (*Helianthus annuus* L.) under well-watered and water-limited conditions. PLoS One **13**, e0204279.

Messier J, Lechowicz MJ, McGill BJ, Violle C, Enquist BJ. 2017. Interspecific integration of trait dimensions at local scales: the plant phenotype as an integrated network. Journal of Ecology **105**, 1775–1790.

Meyer RC, Gryczka C, Neitsch C, Müller M, Bräutigam A, Schlereth A, Schön H, Weigelt-Fischer K, Altmann T. 2019. Genetic diversity for nitrogen use efficiency in *Arabidopsis thaliana*. Planta **250**, 41–57.

Milla R, Bastida JM, Turcotte MM, *et al*. 2018. Phylogenetic patterns and phenotypic profiles of the species of plants and mammals farmed for food. Nature Ecology & Evolution **2**, 1808–1817.

Mural RV, Grzybowski M, Miao C, *et al*. 2021. Meta-analysis identifies pleiotropic loci controlling phenotypic trade-offs in sorghum. Genetics **218**, iyab087.

Nissen KS, Willats WGT, Malinovsky FG. 2016. Understanding CrRLK1L function: cell walls and growth control. Trends in Plant Science **21**, 516–527.

Pigliucci M, Preston K. 2004. Phenotypic integration: studying the ecology and evolution of complex phenotypes. Oxford: Oxford University Press.

Poorter H, Anten NPR, Marcelis LFM. 2013. Physiological mechanisms in plant growth models: do we need a supra-cellular systems biology approach? Plant, Cell & Environment **36**, 1673–1690.

Poorter H, Knopf O, Wright IJ, Temme A, Hogewoning SW, Graf A, Cernusak LA, Pons TL. 2021. A meta-analysis of responses of C_3 plants to atmospheric CO_2: dose–response curves for 85 traits ranging from the molecular to the whole plant level. New Phytologist **233**, 1560–1596.

Poorter H, Niinemets U, Ntagkas N, Siebenkäs A, Mäenpää M, Matsubara S, Pons T. 2019. A meta-analysis of plant responses to light intensity for 70 traits ranging from molecules to whole plant performance. New Phytologist **223**, 1073–1105.

Ramankutty N, Mehrabi Z, Waha K, Jarvis L, Kremen C, Herrero M, Rieseberg LH. 2018. Trends in global agricultural land use: implications for environmental health and food security. Annual Review of Plant Biology **69**, 789–815.

R Core Team. 2021. R: a language and environment for statistical computing. Vienna: R Foundation for Statistical Computing.

Richards CL, Bossdorf O, Muth NZ, Gurevitch J, Pigliucci M. 2006. Jack of all trades, master of some? On the role of phenotypic plasticity in plant invasions. Ecology Letters **9**, 981–993.

Robertson GP, Vitousek PM. 2009. Nitrogen in agriculture: balancing the cost of an essential resource. Annual Review of Environment and Resources **34**, 97–125.

RStudio Team. 2021 RStudio: integrated development environment for R. Boston, MA: RStudio, PBC.

Sauer M, Robert S, Kleine-Vehn J. 2013. Auxin: simply complicated. Journal of Experimental Botany **64**, 2565–2577.

Schneider CA, Rasband WS, Eliceiri KW. 2012. NIH Image to ImageJ: 25 years of image analysis. Nature Methods **9**, 671–675.

Schneiter AA, Miller JF. 1981. Description of sunflower growth stages. Crop Science **21**, 901–903.

Seethepalli A, Dhakal K, Griffiths M, Guo H, Freschet GT, York LM. 2021. RhizoVision explorer: open-source software for root image analysis and measurement standardization. AoB Plants **13**, lab056.

Stahlhut KN, Dowell JA, Temme AA, Burke JM, Goolsby EW, Mason CM. 2021. Genetic control of arbuscular mycorrhizal colonization by *Rhizophagus intraradices* in *Helianthus annuus* (L.). Mycorrhiza **31**, 723–734.

Svensson EI, Arnold SJ, Bürger R, *et al*. 2021. Correlational selection in the age of genomics. Nature Ecology & Evolution **5**, 562–573.

Swarbreck SM, Wang M, Wang Y, Kindred D, Sylvester-Bradley R, Shi W, Varinderpal-Singh Bentley AR, Griffiths H. 2019. A roadmap for lowering crop nitrogen requirement. Trends in Plant Science **24**, 892–904.

Tegeder M, Masclaux-Daubresse C. 2018. Source and sink mechanisms of nitrogen transport and use. New Phytologist **217**, 35–53.

Temme AA, Kerr KL, Masalia RR, Burke JM, Donovan LA. 2020. Key traits and genes associate with salinity tolerance independent from vigor in cultivated sunflower. Plant Physiology **184**, 865–880.

Temme AA, Kerr KL, Nolting KM, Dittmar EL, Masalia RR, Bucksch AK, Burke JM, Donovan LA. 2024. Data from: The genomic basis of nitrogen utilization efficiency and trait plasticity to improve nutrient stress tolerance in cultivated sunflower. Zenodo: https://doi.org/10.5281/zenodo.10137780

Tilman D, Balzer C, Hill J, Befort BL. 2011. Global food demand and the sustainable intensification of agriculture. Proceedings of the National Academy of Sciences, USA **108**, 20260–20264.

Todesco M, Owens GL, Bercovich N, *et al*. 2020. Massive haplotypes underlie ecotypic differentiation in sunflowers. Nature **584**, 602–607.

Tran VH, Temme AA, Donovan LA. 2020. Wild and cultivated sunflower (*Helianthus annuus* L.) do not differ in salinity tolerance when taking vigor into account. Agronomy **10**, 1013.

Venables WN, Ripley BD. 2003. Modern applied statistics with S. New York: Springer.

Vitousek PM, Aber JD, Howarth RW, Likens GE, Matson PA, Schindler DW, Schlesinger WH, Tilman DG. 1997. Human alteration of the global nitrogen cycle: sources and consequences. Ecological Applications **7**, 737–750.

Wagner GP, Zhang J. 2011. The pleiotropic structure of the genotype–phenotype map: the evolvability of complex organisms. Nature Reviews. Genetics **12**, 204–213.

Walsh B, Blows MW. 2009. Abundant genetic variation + strong selection = multivariate genetic constraints: a geometric view of adaptation. Annual Review of Ecology, Evolution, and Systematics **40**, 41–59.

Weih M, Hamnér K, Pourazari F. 2018. Analyzing plant nutrient uptake and utilization efficiencies: comparison between crops and approaches. Plant and Soil **430**, 7–21.

Wright IJ, Reich PB, Westoby M, *et al*. 2004. The worldwide leaf economics spectrum. Nature **428**, 821–827.

Xu G, Fan X, Miller AJ. 2012. Plant nitrogen assimilation and use efficiency. Annual Review of Plant Biology **63**, 153–182.

Zhao X, Nie G, Yao Y, Ji Z, Gao J, Wang X, Jiang Y. 2020. Natural variation and genomic prediction of growth, physiological traits, and nitrogen-use efficiency in perennial ryegrass under low-nitrogen stress. Journal of Experimental Botany **71**, 6670–6683.

Zhou X, Stephens M. 2014. Efficient multivariate linear mixed model algorithms for genome-wide association studies. Nature Methods **11**, 407–409.